Received: 14 May 2021 | Revised: 3 September 2021 | Accepted: 19 September 2021

DOI: 10.1002/bit.27941

ARTICLE

BIOTECHNOLOGY AND BIOENGINEERING WILEY

# Magnetic levitation assisted biofabrication, culture, and manipulation of 3D cellular structures using a ring magnet based setup

Muge Anil-Inevi[1] | Kerem Delikoyun[1] | Gulistan Mese[2] | H. Cumhur Tekin[1] | Engin Ozcivici[1]

[1]Department of Bioengineering, Izmir Institute of Technology, Izmir, Turkey

[2]Department of Molecular Biology and Genetics, Izmir Institute of Technology, Izmir, Turkey

**Correspondence**
Engin Ozcivici, Department of Bioengineering, Izmir Institute of Technology, Urla 3543, Izmir, Turkey.
Email: enginozcivici@iyte.edu.tr

**Funding information**
Türkiye Bilimsel ve Teknolojik Arastirma Kurumu, Grant/Award Number: 119M755

## Abstract

Diamagnetic levitation is an emerging technology for remote manipulation of cells in cell and tissue level applications. Low-cost magnetic levitation configurations using permanent magnets are commonly composed of a culture chamber physically sandwiched between two block magnets that limit working volume and applicability. This work describes a single ring magnet-based magnetic levitation system to eliminate physical limitations for biofabrication. Developed configuration utilizes sample culture volume for construct size manipulation and long-term maintenance. Furthermore, our configuration enables convenient transfer of liquid or solid phases during the levitation. Before biofabrication, we first calibrated/ the platform for levitation with polymeric beads, considering the single cell density range of viable cells. By taking advantage of magnetic focusing and cellular self-assembly, millimeter-sized 3D structures were formed and maintained in the system allowing easy and on-site intervention in cell culture with an open operational space. We demonstrated that the levitation protocol could be adapted for levitation of various cell types (i.e., stem cell, adipocyte and cancer cell) representing cells of different densities by modifying the paramagnetic ion concentration that could be also reduced by manipulating the density of the medium. This technique allowed the manipulation and merging of separately formed 3D biological units, as well as the hybrid biofabrication with biopolymers. In conclusion, we believe that this platform will serve as an important tool in broad fields such as bottom-up tissue engineering, drug discovery and developmental biology.

KEYWORDS
biofabrication, cellular spheroids, magnetic levitation, scaffold free, stem cells

## 1 | INTRODUCTION

Magnetic force-based manipulation of the living cells has emerged as a powerful tool for cellular and tissue level bioengineering applications (Castro & Mano, 2013; Pan et al., 2012; Yaman et al., 2018; Zhao et al., 2016). With the advances in technology and the improvements in design, magnetic manipulation systems with different complexity have been developed for various biotechnological goals including isolation and enrichment of rare cells (Chen et al., 2015; Zeng et al., 2015) and guiding cells into a particular spatial arrangement in two dimensional (2D) or three dimensional (3D) cultures (Ino et al., 2009; Mattix et al., 2014; Whatley et al., 2014). Compared to the alternative operation principles such as

  

electrical, optical and acoustic force-based techniques, magnetic manipulation offers various advantages such as minimal impact on cell viability, simple and low-cost design, and low sensitivity to environmental parameters such as ionic concentration and pH (Nam-Trung, 2012).

Cell magnetophoresis can be performed in two ways, either by manipulating the magnetic susceptibility of the cells or manipulating the magnetic susceptibility of the environment that cells are found (Pan et al., 2012; Yaman et al., 2018; Zhao et al., 2016). Cells, that exhibit greater magnetic susceptibility than their surrounding buffer or medium due to labeling with magnetic particles or a rare intrinsic property of some cell types (i.e., paramagnetic hemoglobin containing red blood cells and magnetotactic bacteria), move towards regions of the high magnetic field (positive magnetophoresis) (Pamme, 2006). However, most cell types are diamagnetic in nature, and once placed into a surrounding environment with high magnetic susceptibility, they are repelled towards the minimal magnetic field (negative magnetophoresis, also referred to as diamagnetophoresis) (Anil-Inevi et al., 2019b; Durmus et al., 2015; Sarigil et al., 2019a, 2019b; Winkleman et al., 2004). Stable cell trapping and self-assembly have been previously conducted by both positive and negative magnetophoresis to create viable 3D structures (Anil-Inevi et al., 2018; Haisler et al., 2013; Sarigil et al., 2020). In positive magnetophoresis, it is possible to manipulate cells even with extremely small magnetic gradients using magnetic labels, allowing cell culture to reach high volume ratios up to several milliliters (Jeong et al., 2016; Souza et al., 2010). However, this manipulation technique is challenging because labeling process is time-consuming and manually intensive (Robert et al., 2011) as well as prone to experimental variability based on variations in magnetic moments of beads (Tarn et al., 2009) or cell labeling efficiency (Jing et al., 2008).

Negative magnetophoresis-based magnetic levitation of cells in contrast, benefits from a label-free methodology. This approach was conventionally performed under a strong magnetic field generated by electromagnets due to the low magnetic susceptibility difference between the biological material and its surroundings (Simon & Geim, 2000). Recently, label-free magnetophoresis has been successfully applied in combination with another external force (Parfenov et al., 2020) or alone (Parfenov et al., 2020) to form complex structures of different sizes and shapes in a high magnetic field. As a simple and low-cost alternative, permanent magnets have been recently used to levitate diamagnetic objects in paramagnetic salt solutions or ferrofluids under weak magnetic fields (Mirica et al., 2010, 2011; Zhao et al., 2016). A magnetic levitation configuration was proposed to levitate diamagnetic objects based on their physical properties. This system levitates materials in paramagnetic solutions under a low magnetic field (<0.5 T) that is generated by two rectangular permanent magnets with the same poles facing each other (Anil-Inevi et al., 2019b; Durmus et al., 2015; Mirica et al., 2009). However, this setup only allows biofabrication applications in microcapillaries, limiting working volumes for cells (Anil-Inevi et al., 2018, 2019a; Sarigil et al., 2020; Türker et al., 2018). Increasing the size of living structures is of prime importance for straightforward implementation of testing protocols by providing an adequate number of cells (Menasche et al., 2019; Shen et al., 2017; Van Peer et al., 2012), and for the production of sizable tissue engineering constructs (Morrison et al., 2016; Park et al., 2019). A technique has been previously reported showing that large nonliving objects (9 mm in length) can be levitated between two square (5.0 × 5.0 × 2.5 cm) or disc (4.8 cm in diameter, 2.5 cm thick) permanent Neodymium (NdFeB) magnets larger than in microfluidic setups (Subramaniam et al., 2014). This technique has been then adapted to levitate millimeter-sized objects including living cell-laden beads and hydrogel units (Tasoglu et al., 2015b). However, these configurations require the assembly of 2 NdFeB magnet blocks that constantly exert opposing forces on the system that hinders the technological translation of these setups for long-term usage. Furthermore, opposing magnets constrain the physical boundaries of the setup, limiting the access to the media for proper cell manipulation.

Recently, a ring magnet-based magnetic levitation configuration has been demonstrated for the density-based characterization of nonliving objects (Zhang et al., 2018). This configuration is composed of a single ring magnet and a glass tube of a paramagnetic solution, that are placed coaxially to each other, to provide better visualization and manipulation than that of the two-magnet configurations. Further, levitation systems composed of a pair of ring magnets with the same-poles facing have been proposed to engineer a linear, axially symmetric magnetic field for levitation and density-based analysis of nonliving and living objects (Ge & Whitesides, 2018; Zhang et al., 2019, 2020). Another magnetic installation containing a glass cuvette placed on an axial hole of two upright ring-shaped neodymium magnets with like poles facing each other was used for magnetic levitation of tissue spheroids in a paramagnetic medium (Parfenov et al., 2018). Although these system designs allow for a satisfying visualization of cell constructs, long-term culture of large living structures in a small culture volume, and performing routine cell culture operations such as media refreshment and recovery of samples, especially for mechanically unstable structures require additional considerations and remain untested.

Here, we showed the applicability of a one-step single ring magnet-based magnetic levitation design in formation and culture of 3D living structures. The system was shown to enable living cells to create large self-assembled 3D structures by preserving the cell viability and to allow mass transfers required for maintenance of the cell culture and combining biological units. We reported that the technique could be adapted for culture of several cell types and allowed transfer into intra-matrix culture. To the best of our knowledge, this is the first attempt to adapt a ring magnet-based magnetic levitation system for biofabrication of biological units and combining them.

## 2 | MATERIALS AND METHODS

### 2.1 | Design of magnetic levitation system

Magnetic levitation system is composed of a ring high grade (N52) neodymium (NdFeB) magnet (1″ od × 5/16″ id × 1/4″ thick, K&J Magnetics) and a cell culture tube positioned in the hole of the magnet (Figure 1). The bottom of the cell culture chamber is attached to the hole of the ring

magnet with glue pads or the chamber is fixed on the magnet with a scaled photoreactive resin piece (Clear v2 FLGPCL02) printed using 3D printer (Formlabs Form 2). In the system, gadolinium ($Gd^{3+}$) in the medium creates a difference ($\Delta_\chi = X_c - X_m$) between magnetic susceptibility of the medium ($X_m$) and cells' ($X_c$) to provide the levitation of cells where the magnetic force ($F_{mag}$, Equation 1) acting on cells and the force of gravity ($F_g$, Equation 2) balance each other.

$$\mathbf{F_{mag}} = \frac{V \cdot \Delta\chi}{\mu_o}(\mathbf{B} \cdot \nabla)\mathbf{B} \quad (1)$$

$$\mathbf{F_g} = V\Delta\rho g \quad (2)$$

with V the volume of the cell, $\mu_o$ the permeability of free space ($1.257 \times 10^{-6}$ kg·m·A$^{-2}$·s$^{-2}$), **B** the magnetic induction (in Tesla, T), $\nabla$ the del operator, $\Delta\rho$ the density difference between cell and paramagnetic medium ($\rho_c - \rho_m$) and g the gravitational acceleration (9.8 m·s$^{-2}$). Magnetic induction (**B**) in our magnetic levitation system was simulated by finite element method. For simulations, residual induction value ($B_r$) is assumed as 1.48 T according to the product specifications. Molar magnetic susceptibility of the paramagnetic agent is $3.2 \times 10^{-4}$ M$^{-1}$ and cell diameter is taken as 20 µm. Since the magnitude of $X_m$ is much larger than that of $X_c$, the magnetic susceptibility of diamagnetic cells is negligible.

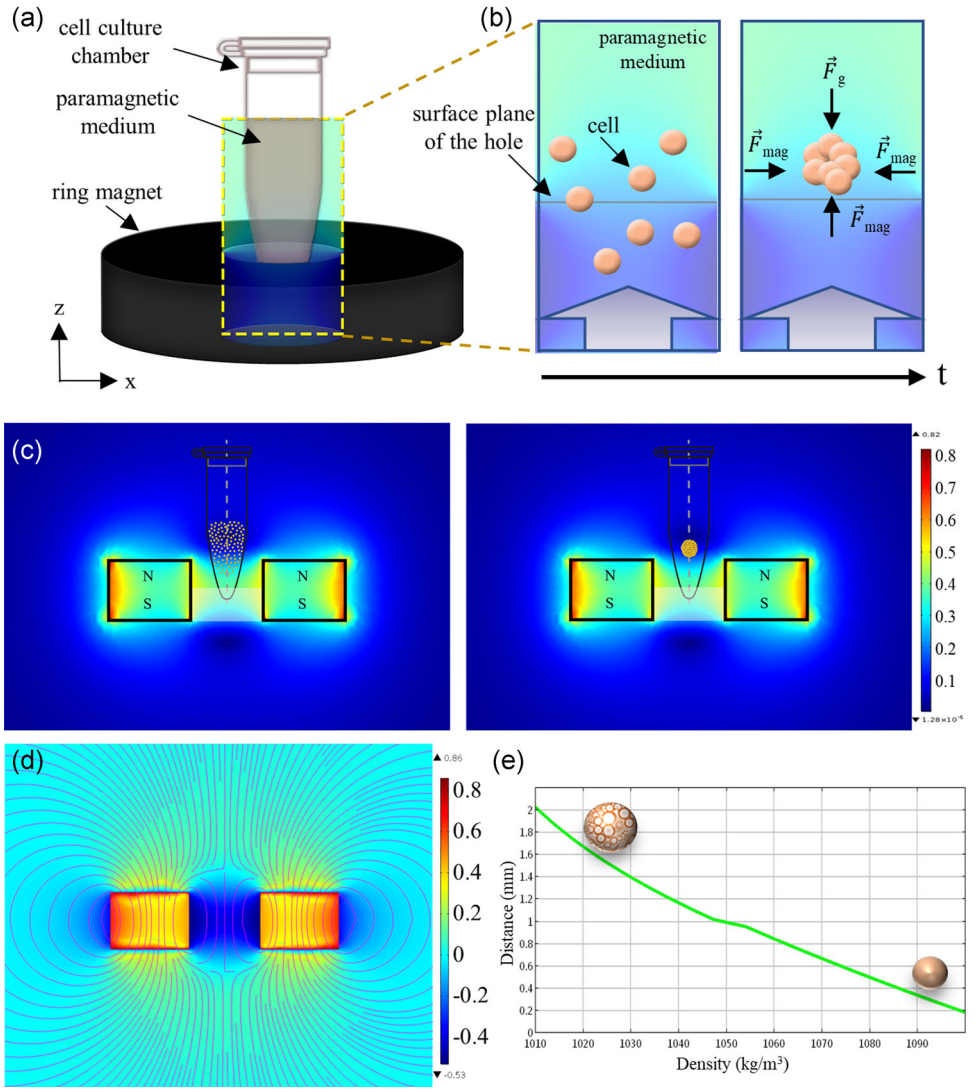


**FIGURE 1** Magnetic force guided levitation and self-assembly. (a) Illustration of magnetic levitation system. Cell culture chamber is positioned on the ring magnet with the bottom of the chamber attached to the hole of the magnet. (b) Schematic representation of the cellular aggregation. The block arrows in the illustration represent upward magnetic induction. (c) Cellular aggregation represented on the simulation of magnetic flux density norm around the ring magnet. (d) Simulation of z component ($B_z$) of magnetic flux density around the ring magnet via finite element methodology. Total magnetic induction ($B_z + B_x$) is presented as streamlines. (e) Modeled relationship between the cell density and levitation heights for 200 mM concentration of $Gd^{3+}$ based on the computational model. Level of the magnet surface is considered as $z = 0$. Density of cells as a function of their lipid content determines levitation height, and while less dense adipocytes are positioned at a higher level, denser cells are positioned at a lower level

In the x-direction, the magnetic forces directed to the centerline enables the cells to focus on the center for cellular aggregation.

## 2.2 | Magnetic levitation of polymeric beads

Polymer beads with densities of 1.02 g/ml (size: 10–20 μm) and 1.09 g/ml (size: 20–27 μm) (Cospheric LLC., ABD), were suspended in the cell culture medium containing 0, 100, and 200 mM $Gd^{3+}$ (Gadavist®; Bayer). Polymer bead suspension was loaded to a micro-capillary channel (1 × 1 mm square cross-section, 50-mm length; Vitrocom) and the channel was positioned on surface of the ring magnet by passing it over the hole of the magnet. That is to say the surface plane of the ring magnet serves as a ground for the levitation process. Movement of the beads in the magnetic field gradient was visualized under a stereo microscope (Soif Optical Instruments).

## 2.3 | Cell culture

D1 ORL UVA (bone marrow stem cell line, American Type Culture Collection [ATCC]) and MDA-MB-231 (breast cancer cell line, ATCC) cells were cultured in Dulbecco's modified Eagle medium (Gibco) supplemented with 10% fetal bovine serum (FBS) and 1% penicillin/streptomycin. 7F2 (mouse osteoblasts, ATCC) cells were cultured in alpha modified essential medium supplemented with 10% FBS and 1% penicillin/streptomycin. The cells were grown in a humidified 37°C incubator with 5% $CO_2$. The growth medium was refreshed every other day and the cells were passaged every 4–6 days. For adipogenic induction, 7F2 cells were exposed to induction medium composed of 5 μg/ml insulin, 10 nM dexamethasone and 50 mM indomethacin for 7 days. The induction medium was refreshed every other day. The cells were observed under an inverted microscope (Olympus IX-83).

## 2.4 | Levitation of living cells

The cells were detached with 0.25% trypsin-ethylenediaminetetraacetic acid when the culture reached near confluency. Following centrifugation and removal of the supernatant, the cells were resuspended to $10^6$ cells/ml in the culture medium with various $Gd^{3+}$ concentrations (50, 100, 150, and 200 mM). A total of 200 μl of cell suspension was loaded into the cell culture tube unless otherwise noted, and the culture tube was placed in the hole of the ring magnet. The cells were levitated in the magnetic levitation system for 24 h and imaged by a mobile phone equipped with a ×15 micro focal length lens (Baseus) for short distance focusing. Horizontal diameter, vertical diameter, area and perimeter of the self-assembled clusters were measured with the ImageJ Fiji software.

## 2.5 | Visualization of trapping region for cellular cluster in the magnetic levitation system

D1 ORL UVA cells were resuspended to $10^6$ cells/ml in the culture medium with 200 mM $Gd^{3+}$ and 100 μl of cell suspension was loaded into the cell culture chamber. Self-assembled cellular cluster after 48 h of levitation was moved upward and downward with the culture chamber to visualize cell trapping region in the vertical plane. For visualization of trapping region in the horizontal plane, the cell culture chamber was positioned horizontally on the ring magnet and moved parallel to the magnet surface until it passed the region where the movement of the cellular cluster was restricted. The motion of the cellular cluster was recorded by a mobile phone equipped with a ×15 micro focal length lens.

## 2.6 | Modification of the medium and magnetic field

Ficoll® PM 400 (Sigma-Aldrich) was added to the culture medium to adjust the density of the medium to 1.02 and 1.04 g/ml. D1 ORL UVA cells ($10^6$ cells/ml) were suspended in the denser culture media with 0 or 100 mM $Gd^{3+}$. Levitation of cells in 200 μl was observed after 24 h of culture. To further increase the magnetic susceptibility of the medium and thus the magnetic force on cells, levitation culture of D1 ORL UVA cells ($10^6$ cells/ml) was performed with increasing concentrations of $Gd^{3+}$; 0, 200, 350, and 500 mM. Levitation and aggregation of cells were observed within 5 h. Two magnets have been attached with their opposite poles facing to strengthen the magnetic field in the levitation system. D1 ORL UVA cells were suspended in paramagnetic medium (150 or 200 mM $Gd^{3+}$) at a concentration of $10^6$ cells/ml and levitated on holes of one ring magnet or two ring magnets whose opposite poles attached to each other. A total of 200 μl of suspension was placed on levitation systems and cultures were observed after 2, 24, and 48 h.

## 2.7 | Transfer of cellular cluster and culture medium in magnetic levitation system

D1 ORL UVA cells were suspended in paramagnetic medium at a final concentration of $10^6$ cells/ml and 200 μl of cell suspension was cultured in magnetic levitation system for 48 h. To refresh the medium, old medium was removed with a pipette and fresh paramagnetic medium was slowly added to the culture.

To show the transfer of the resultant 3D culture, self-assembled compact clusters were harvested from the levitation culture without dispersion with a 1000 μl pipette tip. Harvested clusters were transferred to another levitation culture without dispersion with a 1000 μl pipette tip. All of the operations were recorded by a mobile phone equipped with a ×15 micro focal length lens.

For culture maintenance of cellular cluster formed with magnetic levitation system in culture dish, D1 ORL UVA cells ($10^6$ cells/ml)

were levitated in 200 mM $Gd^{3+}$ containing paramagnetic medium for 48 h and transferred to a culture dish with Gd-free medium. The culture was maintained for 24 h for observation.

## 2.8 | Live/dead assay

D1 ORL UVA cells were suspended in 200 mM $Gd^{3+}$ containing paramagnetic medium and assembled in the magnetic levitation system. The levitation culture was maintained for 48 h before cell viability test. For viability test of the adipogenesis induced 3D structures, adipogenesis induced 7F2 cells were assembled in the magnetic levitation system for 24 h, then transferred to a culture plate and cultured for another 24 h. The viability of cells was assessed using live/dead assay (calcein-AM/propidium iodide, Sigma Aldrich) according to the manufacturer's protocol. The cells were stained for 15 min at 37°C. Images were acquired using a fluorescence microscope (Olympus IX-83). The cells were both investigated as 3D cluster form and as dissociated single cells.

## 2.9 | Co-levitation culture

D1 ORL UVA cells were assembled and maintained during levitation by ring magnet-based magnetic levitation system for 48 h. The self-assembled spheres were transferred one by one to a medium containing 200 mM $Gd^{3+}$ in magnetic levitation system using a micropipette for co-levitation culture. Transfer of the clusters into the co-levitation culture was recorded by a mobile phone. For the co-levitation of 3D clusters consisting of lipid accumulated 7F2 cells, adipogenesis-induced cells were levitated in $Gd^{3+}$-containing media at increasing concentrations (100, 150, and 200 mM) for 24 h, and the clusters were co-levitated in the same Gd-content medium in duplicate. Following a 24-h co-levitation culture, the 3D structures were transferred to the cell culture petri dish and observed under an inverted microscope (Olympus IX-83). Merged areas of each pair of spheres (%) were measured with ImageJ Fiji software by thresholding, followed by shape completion and particle analysis.

## 2.10 | Embedding the 3D structures within the gel matrix

D1 ORL UVA cells were suspended in 200 mM $Gd^{3+}$ containing medium and assembled in the magnetic levitation system for 24 h. At the end of the 24 h of the culture, the medium was aspirated until only 20 µl remained in the culture dish for maintenance of the levitation. Matrigel (BD Biosciences) with five times the volume of the remaining medium, was slowly added to the culture at +4°C and the culture was kept in a humidified 37°C incubator for 3 h. After the Matrigel polymerized, the 3D cell structure in the gel was transferred to a culture plate with the help of a pipette tip, which was cut on one side and turned into a micro spoon. Embedding the 3D structures within Matrigel and transfer of the clusters in Matrigel were recorded by a mobile phone. The medium was added onto the 3D structure embedded in Matrigel in culture dish and cultured for 4 days.

## 2.11 | Statistical analysis

All experiments were repeated at least three times. Results are reported as mean ± *SD*. Statistical analyses were performed using Student's *t* test (two-tail) or two-way analysis of variance with Sidak post hoc correction, with GraphPad Prism version 6.0 (GraphPad Software). A $p$ value of <5% was considered significant.

# 3 | RESULTS

## 3.1 | Self-assembly of living cells in ring magnet-based magnetic levitation

A magnetic levitation system composed of a NdFeB (grade N52) ring magnet and a cell culture chamber was designed for levitation and self-assembly of cells (Figure 1a–d). First, we demonstrated that the system enabled levitation for the density range of the cells, 1.02–1.9 g/ml, and that the cells were localized at 0.3–1.7 mm distance from the magnet surface that was inversely proportional to their density based on the computational simulation (Figure 1e). To demonstrate the applicability of the ring magnet system for the levitation of cells, polymeric beads with a density of 1.02 and 1.09 g/ml, representing the density of less dense and dense cells (Durmus et al., 2015; Sarigil et al., 2019b), respectively, were suspended in paramagnetic solution containing $Gd^{3+}$ (100 and 200 mM), and their movements on the ring magnet were monitored (Figure S1 and Video S1–S6). Polymeric beads with a density of 1.02 g/ml were levitated in paramagnetic media containing both 100 and 200 mM $Gd^{3+}$, while denser particles (1.09 g/ml) were levitated in the medium containing 200 mM $Gd^{3+}$, as they showed sedimentation at 100 mM $Gd^{3+}$ concentration. After demonstrating that the system was able to provide levitation of particles with a density close to that of living cells, D1 ORL UVA cells were suspended in medium with increased concentrations of $Gd^{3+}$ (0, 50, 100, and 200 mM) and cultured in the levitation system for 24 h (Figure 2). In the control group without $Gd^{3+}$, all of the cells settled without levitation. In the paramagnetic medium containing 50 mM $Gd^{3+}$, no cellular aggregates were formed. During the first 2 h of culture, the beginning of the cell clustering process in the paramagnetic medium with 100 and 200 mM $Gd^{3+}$ concentrations was observable with the naked eye as cloudy aggregation of cells, and after 24 h, compact 3D structures were formed in these groups. While the majority of cells suspended in 100 mM could not be levitated in the system and sedimented to the bottom, cells suspended in 200 mM formed large 3D self-assembled clusters with levitation (Figure 2a, red circles). The average horizontal diameter of cell clusters formed in medium with 200 mM $Gd^{3+}$ was

867.33 ± 94.93 µm and approximately 1.7 times its vertical diameter. Cross-sectional area and perimeter of these clusters were measured as 0.39 ± 0.05 $mm^2$ and 3.52 ± 0.36 mm, respectively (Figure 2b).

Magnetic levitation culture was performed by manipulating the culture medium properties and the magnetic field. To reduce the gravitational force acting on the cells and, therefore, the magnetic susceptibility required to provide levitation, the density of the medium was increased by adding Ficoll to the medium, and D1 ORL UVA cells were levitated in these denser media (Figure S2). When the density of the culture medium was increased to 1.02 g/ml, the medium containing 100 mM $Gd^{3+}$ concentration levitated most cells, unlike 1 g/ml medium. Measured horizontal diameter, vertical diameter, area and perimeter of cellular structures formed in medium with 1.02 g/ml density were 1005.33 ± 123.29 µm, 712 ± 54.03 µm, 0.70 ± 0.13 $mm^2$ and 4.15 ± 1.09 mm, respectively. Moreover, horizontal diameter ($p = 0.73$), vertical diameter ($p = 0.67$), area ($p = 0.24$) and perimeter ($p = 0.82$) of cellular structures formed in medium with 1.02 g/ml density were statistically similar to structures observed with 1 g/ml medium with 200 mM $Gd^{3+}$ concentration. Further increase in the medium density to 1.04 g/ml did not result in observable cluster formation.

To test whether rising the magnetic susceptibility of the medium increased the formation rate of cell clusters, we applied 350 and 500 mM $Gd^{3+}$ concentrations, however no compact 3D structure was formed in none of the groups within 5-h levitation as in the media containing 200 mM $Gd^{3+}$ (Figure S3). Finally, we tested whether changing the strength of magnetic field by increasing lateral magnet area twofold would affect the size of D1 ORL UVA cell clusters (Figure S4a–e). However, biofabricated forms did not have a significant size difference in horizontal diameter ($p = 0.62$ and 0.74, respectively), vertical diameter ($p = 0.50$ and 0.56), area ($p = 0.26$ and 0.22) and perimeter ($p = 0.99$ and 0.57) in the medium containing 150 and 200 mM $Gd^{3+}$. Computational simulation for magnet thickness implied that the system achieved a tighter focusing of cells with increased magnet thickness (Figure S4f).

## 3.2 | Mass manipulation in 3D culture with ring magnet-based magnetic levitation

We next investigated the suitability of ring magnet-based magnetic levitation setup for mass manipulations in cell culture. To visualize cell focusing region in ring magnet-based magnetic levitation in the vertical plane, D1 ORL UVA cluster assembled with magnetic levitation was moved vertically with the culture chamber (Figure 3a and Video S7). Equilibrium position was robustly kept by the cell cluster during the movement of the system in both directions. Next, to observe cell focusing region on the horizontal plane, D1 ORL UVA

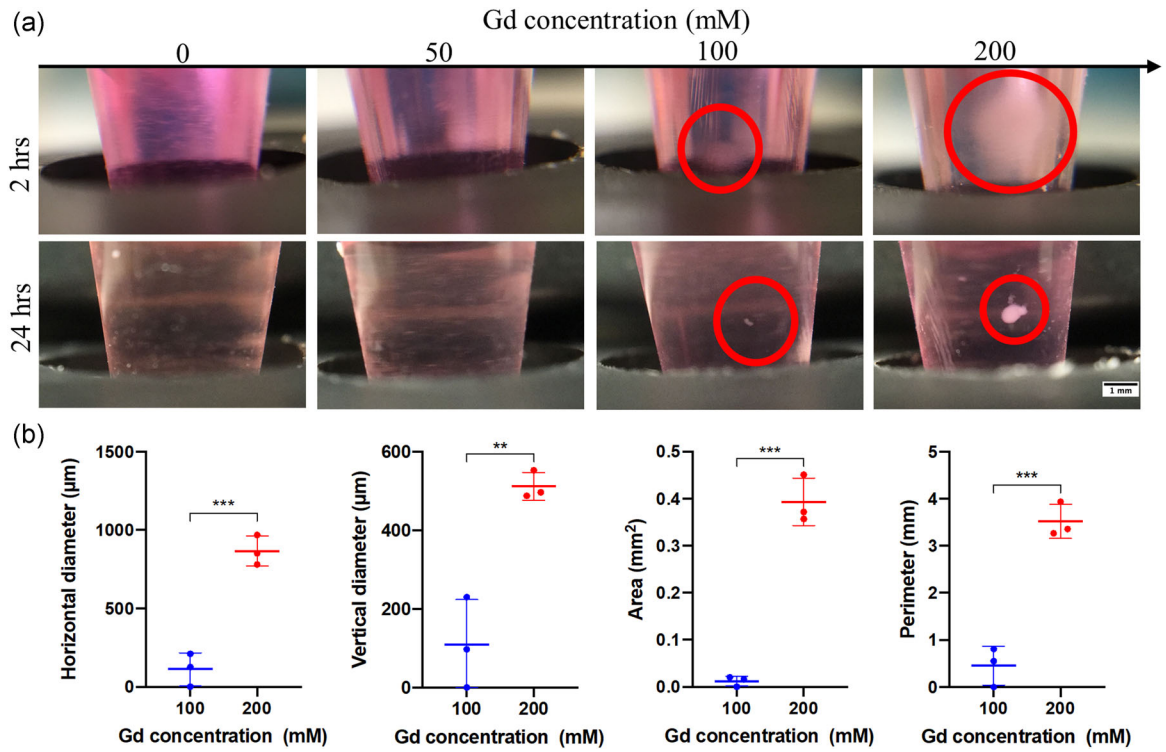


**FIGURE 2** Self-assembly of D1 ORL UVA cells in ring magnet-based magnetic levitation system. (a) Micrographs of D1 ORL UVA cells cultured with ring magnet-based magnetic levitation (0, 50, 100, and 200 mM $Gd^{3+}$, $10^6$ cells/ml, 100 µl) after 2 or 24 h of culture. Scale bar: 1 mm. (b) Size of the cellular clusters formed for 24 h with magnetic levitation (100 and 200 mM $Gd^{3+}$, $10^6$ cells/ml, 100 µl); horizontal diameter, vertical diameter, area and perimeter. Data are plotted as mean of replicates with error bars (±*SD*) and statistical significance was determined by Student's *t* test (two-tail). $^{**}p < 0.01$; $^{***}p < 0.001$

cluster formed by magnetic levitation culture was moved from the center of the magnet to the outside, parallel to the surface of the ring magnet with the culture chamber (Figure 3b and Video S8). When the cellular structure reached the boundary of the area above the hole of the magnet, it was moved back towards the center of the magnet due to the high magnetic field on the magnet surface.

Applicability of the medium refreshment, which is an essential factor for long-term maintenance, was tested during levitation cell cultures that contained self-assembled and 48 h cultured D1 ORL UVA cells (Figure 3c and Video S9). The ring magnet-based magnetic levitation system was found to be suitable for removing and replacing up to 80% of 200 µl total media volume with fresh medium, without causing the cellular cluster to settle. Gentle transfer of the medium using a micropipette ensured that the 3D structure in the system was not damaged. We followed this test of liquid phase transfer by viable cell cluster transfer. 3D structures formed of $2 \times 10^5$ D1 ORL UVA cells were also gently collected from the levitation culture without distortion using a 1000 µl pipette tip (Figure 3d and Video S10). Then, the clusters that were harvested from a levitation culture were found to be transferred to another levitation culture without any distortion (Figure 3e and Video S11).

### 3.3 | Long-term levitation culture

Effects of levitation culture on the health of cells were tested by transferring 3D cellular spheres formed during 24 h of levitation culture to a standard culture dish (Figure 4a and Figure S5). We observed that the cells spread adherently at the edges of the 3D cellular cluster to ~43% of the 3D cluster's diameter for the sphere with a diameter of about 713 ± 3 µm. To determine the viability of the 3D structures formed in the magnetic levitation system, we performed a live/dead assay to both an intact 3D cluster (Figure 4b) as well as to a dissociated form as a single-cell suspension (Figure 4c). Visual inspection of the live/dead fluorescence microscopy images showed that 66% of the cells were viable as apparent from the green calcein-AM signal in both 3D form and the single cell suspension.

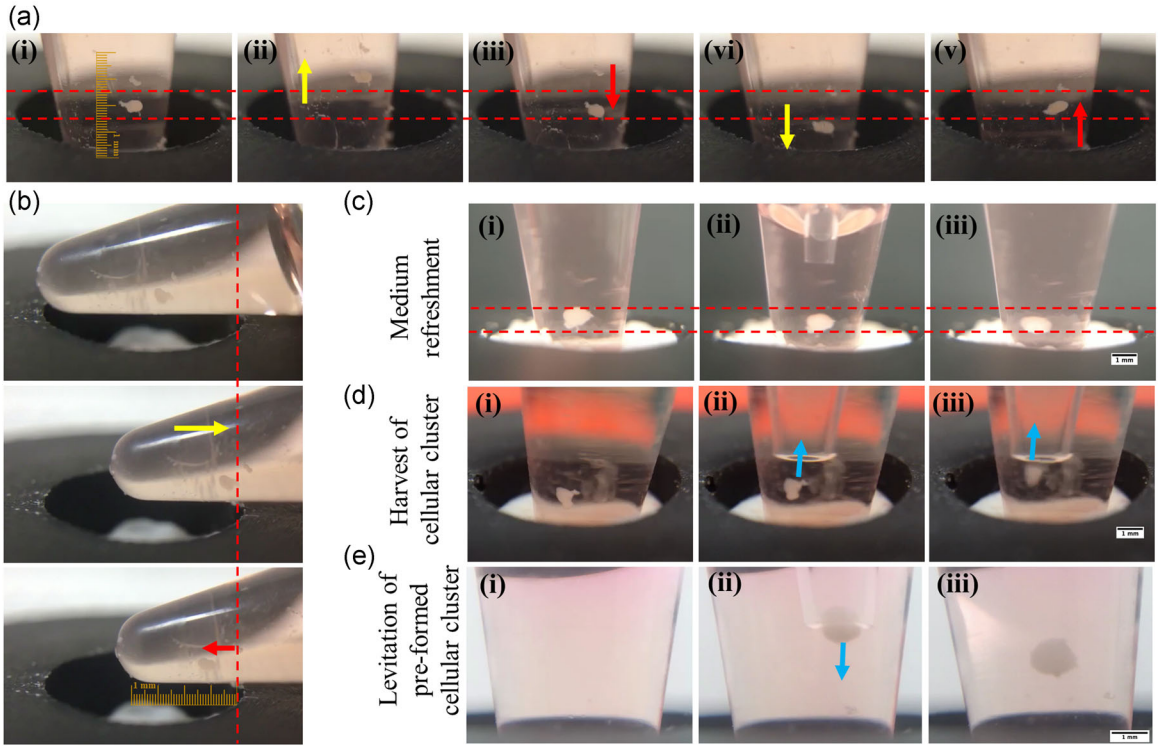


**FIGURE 3** Mass manipulation in 3D culture with ring magnet-based magnetic levitation. (a) Trapping region of self-assembled D1 ORL UVA cluster (200 mM $Gd^{3+}$, $10^6$ cells/ml, 100 µl) in the magnetic levitation system; (a) in the vertical plane, (b) in the horizontal plane. When the cellular cluster at equilibrium position (i) was moved upward with the culture chamber (ii), the cluster fell down into the equilibrium position (iii). When the cellular cluster was moved downward with the culture chamber (iv), the cluster rose back to its equilibrium position (v). Between the red dashed lines indicate the region in which the cellular cluster tends to be balanced in figure (a). The red dashed line indicates the limit of the region in which the cellular cluster remains in the horizontal plane in figure (b). Yellow arrows show the direction, which the cellular cluster is moved with the culture chamber as an external force, and the red arrows show the direction which the cellular cluster inherently moves. (c) Refreshing culture medium of 3D cellular cluster formed in the magnetic levitation system (200 mM $Gd^{3+}$, $10^6$ cells/ml, 200 µl) at the equilibrium position (i); removal of old medium (ii) and addition of fresh medium (iii). (d) Harvest of a 3D cellular cluster formed in the magnetic levitation system at the equilibrium position (i) by gently aspirating it with a pipette (ii, iii). (d) Transfer of 3D cellular cluster formed in the magnetic levitation system into another magnetic levitation device with a pipette. Scale bars: 1 mm

The potential of the ring magnet-based magnetic levitation system to biofabricate complex structures consisting of 3D living units was demonstrated by successful co-levitation of homocellular spheroids that were levitation cultured and transferred from a prior system (Figure 4d–g). The 3D spheres formed as a result of magnetic levitation of D1 ORL UVA cells were gently transferred into the medium containing 200 mM $Gd^{3+}$ in the levitation system (Figure 4e). Co-levitation cultures formed by transferring two or four of them to the device (Videos S12 and S13) were maintained for another 24 h to allow cell–cell attachment between spheroids. We observed that the cellular spheres were fused after 24 h of co-levitation and they were successfully transferred to a different culture dish without deterioration for a better display of the intercluster contact zones in 3D structures (Figure S6). A 24 h co-levitation resulted in 1.07 ± 0.35% merging of the spheres in area and no statistical difference was observed between percentages of fusion in bilateral and quadruple co-levitation cultures ($p = 0.87$) (Figure 4h and Figure S7).

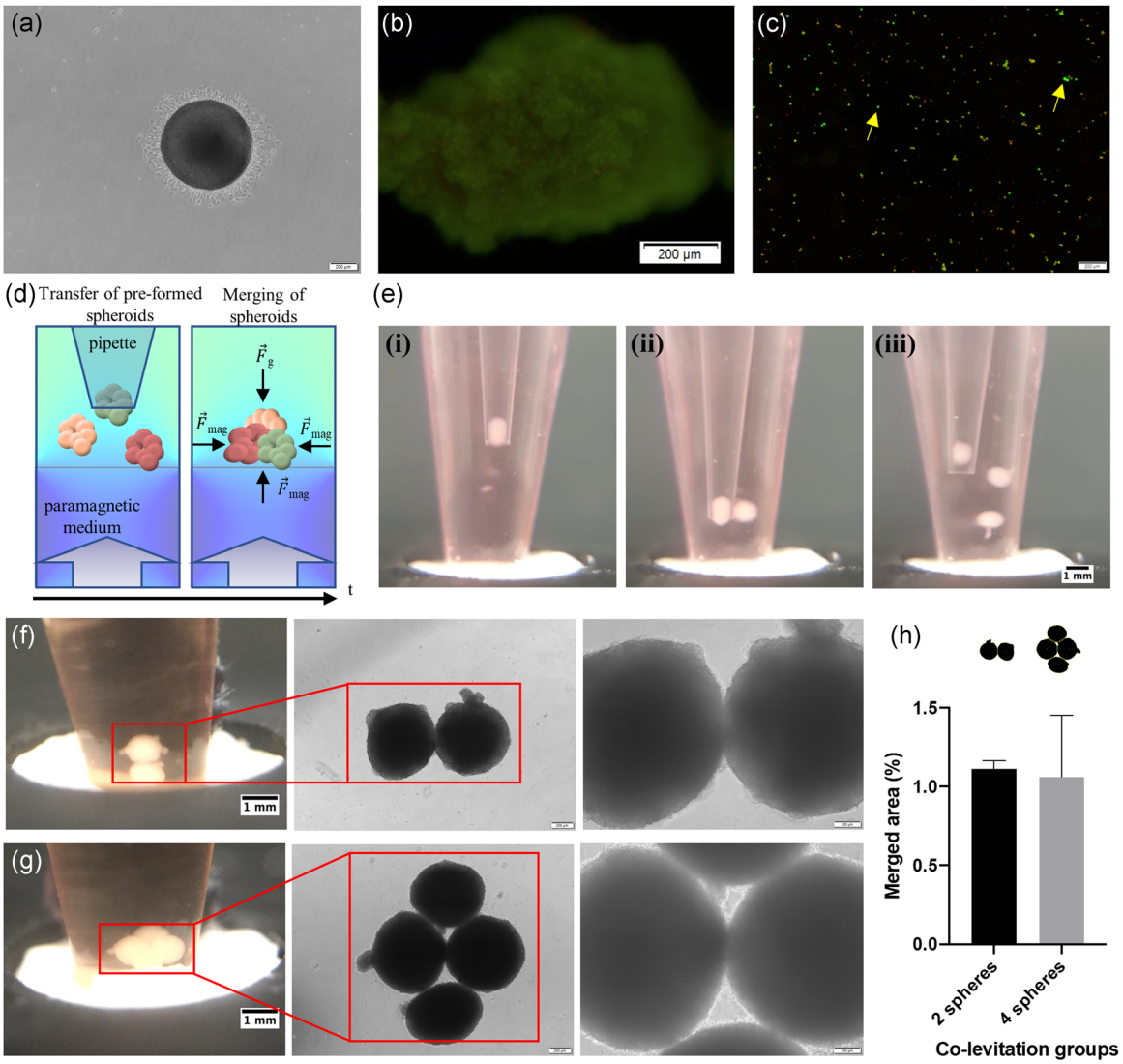


**FIGURE 4** Postoperations on spheres formed by ring magnet-based levitation. (a) Micrograph of a self-assembled D1 ORL UVA 3D structure cultured with magnetic levitation (200 mM $Gd^{3+}$, $10^6$ cells/ml, 200 µl) for 48 h and then cultured for 24 h in the 2D culture dish. Fluorescent microscopy images of D1 ORL UVA (b) 3D structures formed with magnetic levitation and (c) cells dissociated from the 3D structures (live: green, dead: red). Cell viability was visualized by live-dead staining (Calcein/PI). Yellow arrows denote some of the alive cells. Scale bar: 200 µm. (d) Schematic representation of the co-levitation of self-assembled cellular clusters. (e) One-by-one transfer of D1 ORL UVA cellular clusters that were individually self-assembled and cultured for 48 h in ring magnet-based magnetic levitation system to the medium containing 200 mM $Gd^{3+}$ in magnetic levitation system for co-levitation culture. Co-levitation culture of preformed (f) two and (g) four D1 ORL UVA cellular clusters in medium containing 200 mM $Gd^{3+}$ in the magnetic levitation system for 24 h. Scale bars: 1 mm for culture chamber images, 200 and 100 µm for middle and right images, respectively, in (f) and (g). (h) Merged area of spheres (%) co-levitated in a medium containing 200 mM $Gd^{3+}$ for 24 h. Data are plotted as mean of replicates with error bars (±*SD*) and evaluated using the unpaired Student's *t* test

### 3.4 | Magnetically guided self-assembly of cells with different single cell densities

Since one of the features determining the final position of the cells in the magnetic levitation principle is the inherent single cell densities, the levitation-based 3D culture protocol of low-density cells in the system was defined using adipocytes with low density due to cellular lipid accumulation (Sarigil et al., 2019b). Adipogenesis of 7F2 cells was induced for 7 days to obtain lipid accumulated cells (Figure S8). Following the observation of lipid accumulation, the cells were suspended in the paramagnetic medium containing increasing $Gd^{3+}$ concentrations (0, 100, 150, and 200 mM) and levitation cultured over 24 h in the ring magnet-based magnetic levitation system (Figure 5a). We observed that the cells started to accumulate on the magnet towards the center in all paramagnetic medium containing $Gd^{3+}$ between 100 and 200 mM at the second hour of the culture, and these stably levitated cells formed 3D structures at the 24th hour of the culture. The spheres formed in 100 mM $Gd^{3+}$ containing medium were 1.95 and 2.95 times larger in area (~5.8 $mm^2$), and 1.51 and 1.58 times larger in perimeter (~10.72 mm) than those formed in the medium containing 150 and 200 mM $Gd^{3+}$, respectively (Figure 5b). There was no statistically significant difference between the areas ($p = 0.06$) and perimeters ($p = 0.78$) of the clusters formed in the medium containing 150 and 200 mM $Gd^{3+}$. When the cells were assembled in the medium containing 100 mM $Gd^{3+}$, the shapes of the clusters were skewed in the direction of the vertical diameter rather than horizontal diameter compared to the clusters formed in paramagnetic medium containing higher $Gd^{3+}$. Closer inspection of the graph showed that the vertical diameter of the cellular clusters formed in the medium containing 100 mM $Gd^{3+}$ was 3917 ± 622.55 µm and it was 2.38 and 2.72 times more than the clusters formed at 150 mM and 200 mM $Gd^{3+}$ concentrations, respectively.

As the cell density decreases, it is expected that the paramagnetic agent concentration required to levitate the cells decreases due to diminishing gravitational force on cells (Figure S9a). Here, computational simulation was performed for cells with a density of 1.09, 1.06, and 1.02 g/ml to represent cells with high, medium and low density, respectively. The simulation results showed that it was necessary to increase the $Gd^{3+}$ in the medium up to 200 mM to balance the gravitational force acting on the cells with a density of 1.09 g/ml and to achieve levitation of the cells. When the cell density decreases to 1.06 and 1.02 g/ml, 150 and 50 mM $Gd^{3+}$ are sufficient for levitation, respectively. To experimentally test whether a paramagnetic agent concentration lower than 100 mM would provide levitation for the adipocyte population, cells were cultured in the levitation system in media containing 0, 12.5, 25, and 50 mM $Gd^{3+}$. A small population was positioned above the main population in medium containing 50 mM $Gd^{3+}$, probably due to the heterogeneity of lipid accumulation and thus cell densities in the population, however, the entire structure was in contact with the culture surface and was devoid of complete levitation (Figure S9b). Additionally, unlike the others in 50 mM group, the magnetic force caused a circular focusing of the cells (on the x and y axes). In the medium containing 25 mM $Gd^{3+}$ concentration, at the end of 2 h, there was a group of cells with levitation above the main population, while after 24 h, complete sedimentation was observed at all concentrations lower than 50 mM probably since the magnetic force created on the cells at these concentrations was not large enough to balance gravitational force, as in the control group.

To maintain culture of the adipogenesis induced 3D structures, which were formed as a result of 24-h levitation, spheroids were transferred to a culture plate and cultured for another 24 h (Figure S10). We observed that the transferred 3D structures were loose and many adipocytes dissociated from the edges of the 3D clusters in all paramagnetic medium groups after the transfer. While most of the cells separated from the main cluster were in suspended form, some lipid-containing cells were observed to spread over the culture surface. Testing the viability of cells at the end of the culture by live/dead staining showed that most cells in the 3D cluster were alive (Figure 5c and Figure S11). We also carried out co-levitation of 3D adipogenesis-induced cell clusters formed separately in the same medium for 24 h (Figure S12). Although the clusters appeared together with the assistance of magnetic force in the levitation system at the 24th hour of levitation, we observed that there was still no fusion between the clusters when transferred to the culture vessel and the clusters were dispersed with the transfer.

The ring magnet-based magnetic levitation system was also tested for biofabrication of 3D structures of MDA-MB-231 breast cancer cells levitation cultured for 24 h in medium containing 150 and 200 mM $Gd^{3+}$ (Figure 5d). In the second hour of the culture, cell clustering began with a nebulous appearance in the paramagnetic medium and levitated tight 3D clusters with an area of 1.37 ± 0.17 $mm^2$ were observed at the 24th hour (Figure 5e). The horizontal diameter of the 3D structures formed in the media containing 150 mM $Gd^{3+}$ was ~39% higher and the perimeter was ~22% higher than those formed in the medium containing 200 mM $Gd^{3+}$.

### 3.5 | In-gel culture of self-assembled 3D structures

To demonstrate the transferability and the sustainability of self-assembled 3D structures created with magnetic levitation into an in-gel culture, D1 ORL UVA cells were levitation cultured for 24 h and at the end of the culture self-assembled 3D structures were embedded in Matrigel (Figure 6a,b and Video S14). After aspirating most of the levitation medium leaving enough to sustain the levitation of the 3D structure (~20 µl) we slowly added Matrigel to the levitation system. We transferred the Matrigel in a slow rate to the point that the Matrigel volume was five times the volume of the remaining medium. Matrix was added at +4°C that kept it in liquid form and polymerization was achieved by temperature change. It was shown that the levitated cellular structures could be successfully trapped within the Matrigel without any observable deformation. We then transferred the cellular structure within the gel matrix to a separate culture (Figure 6c–e and Video S15). On the 4th day of the culture, we

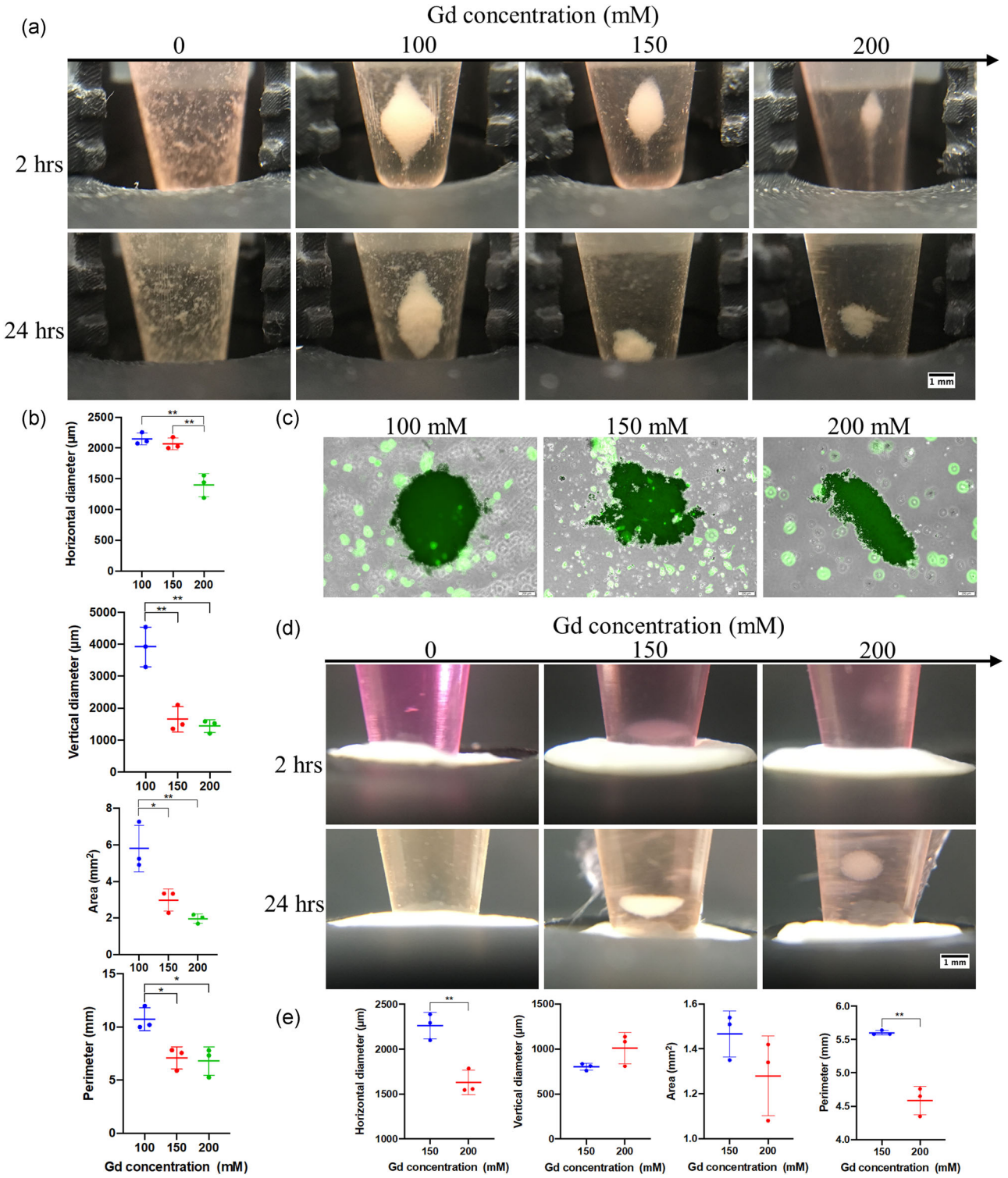


**FIGURE 5** Levitation based 3D culture of different cell types. (a) Micrographs of adipogenesis induced 7F2 cells cultured with ring magnet-based magnetic levitation (0, 100, 150, and 200 mM $Gd^{3+}$, $10^6$ cells/ml, 200 µl) after 2 or 24 h of culture. Each vertical unit on the 3D printed scaled piece: 1 mm. Scale bar: 1 mm. (b) Size of the adipogenesis induced 7F2 cellular clusters formed for 24 h with magnetic levitation; horizontal diameter, vertical diameter, area and perimeter. (c) Fluorescent microscopy images of adipogenesis induced 7F2 3D structures formed with magnetic levitation. Cell viability was visualized by live staining (Calcein-AM). Scale bar: 200 µm. (d) Micrographs of MDA-MB-231 cells cultured with ring magnet-based magnetic levitation (0, 150, and 200 mM $Gd^{3+}$, $10^6$ cells/ml, 200 µl) after 2 or 24 h of culture. Scale bar: 1 mm. (e) Size of the MDA-MB-231 cellular clusters formed for 24 h with magnetic levitation; horizontal diameter, vertical diameter, area and perimeter. Data are plotted as mean of replicates with error bars (±*SD*) and statistical significance was determined by Student's *t* test (two-tail). $^*p < 0.05$; $^{**}p < 0.01$

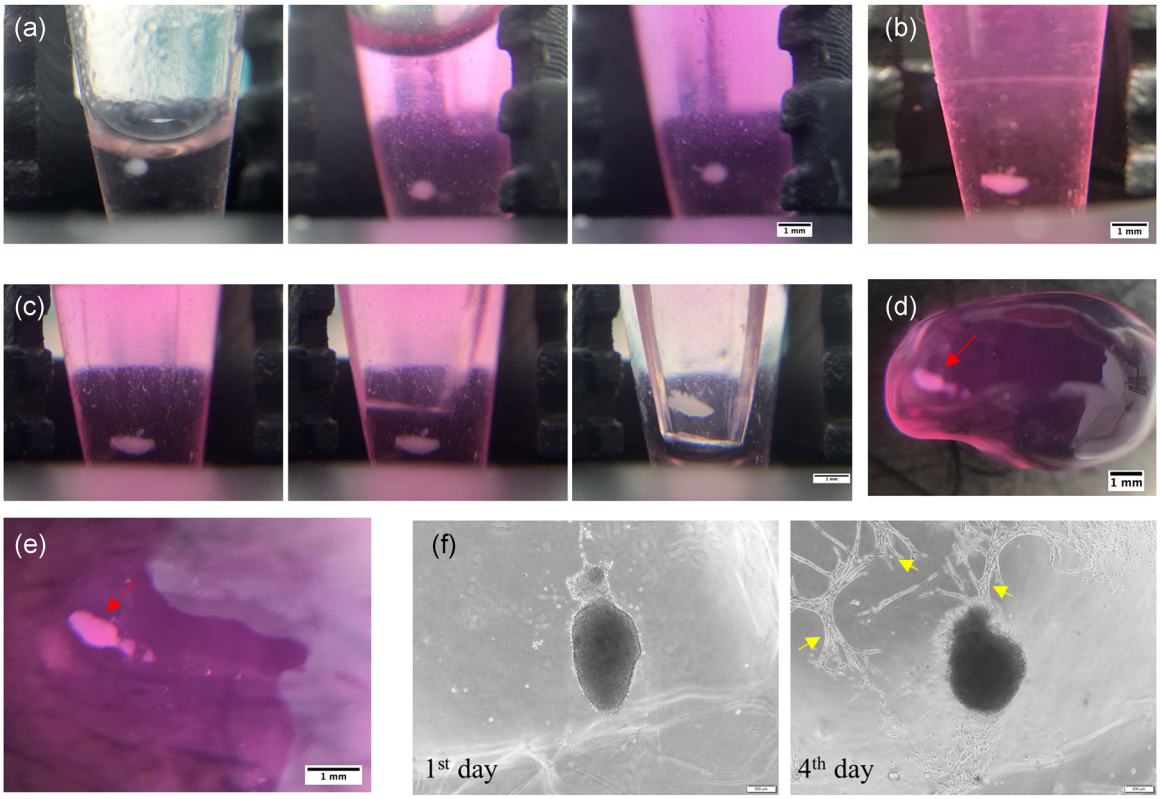


**FIGURE 6** In-gel culture of self-assembled D1 ORL UVA 3D structures. (a) Embedding a 3D cellular structure assembled by magnetic levitation within Matrigel. (b) Cellular cluster in Matrigel at the third hour of culture. (c) Harvest of gel-embedded 3D cluster using a pipette tip, which was cut into a micro-spoon. Matrigel-embedded 3D cluster that was transferred into a culture plate. (d) Before and (e) after medium addition on gel-embedded culture. Red arrows show the 3D clusters in the gel matrix. Each vertical unit on the 3D printed scaled piece: 1 mm. Scale bar: 1 mm (f) Micrographs of the Matrigel-embedded 3D cluster after 1 and 4 days of culture. Yellow arrows indicate some of the cells spreading in the gel matrix. Scale bar: 200 µm

observed that the 3D cellular structure consisted of viable cells spreading in the gel matrix (Figure 6f and Figure S13).

## 4 | DISCUSSION

Magnetic force-assisted cell manipulation provides a broadly applicable guidance tool in many fields such as biological or clinical research and tissue engineering. The availability of label-free protocols has recently led to a greater focus of research on these techniques due to both lowering required cost, time and labor, and enhancing compatibility of the technique for living cells. Some microcapillary based magnetic levitation systems, that were initially applied to detect and sort cells of interest according to their physical intrinsic properties (Baday et al., 2019; Delikoyun et al., 2021; Durmus et al., 2015; Sarigil et al., 2019b; Tasoglu et al., 2015a), were later adapted for biofabrication (Anil-Inevi et al., 2018; Sarigil et al., 2020; Tocchio et al., 2018). While great progress has been made in the field, tissue engineering applications and biological testing protocols require manufacture of sizable living constructs to provide an adequate number of cells. Systems that allow cell culture applications on-site and offer low-cost applications with permanent magnets are essential to render the production easy to install and operate, and to enable on-site intervention to production process.

The standard diamagnetic levitation devices using capillary tubes (1 × 1 mm square cross-section) physically sandwiched between two block permanent magnets are able to create large cellular blocks (up to ~2.68 cm in length) (Anil-Inevi et al., 2018). Although these elongated living structures created in such systems are advantageous in terms of efficient mass transfer between cluster and its surrounding, they are not mechanically resistant to transfer processes due to their low thickness (up to ~280 µm) with low homogeneity towards the capillary ends, limiting their applications in bottom-up tissue engineering. Another magnetic levitation setup design was shown to increase the working volume by positioning larger block magnets (poles on 2 × 2 inch surfaces) further apart with a gap set to 2.5 cm (Tasoglu et al., 2015b). This system allows remote 3D manipulation of millimeter-sized living objects. Such systems still contain opposing magnets occupying the top and bottom of the culture chamber to provide magnetic field gradient required for levitation, and this configuration limits operations on the culture during levitation process such as medium refreshment and transfer of the cellular structures. Ring magnet-based magnetic levitation system proposed here removes the upper physical barrier, hence providing an easy

access to the levitating biological structures and to its surrounding medium. Furthermore, this setup eliminates the limit for the height of the cell culture chamber and thus enables levitation in great height culture containers. We showed that single step axial-circular magnetic levitation made addition and removing of liquid or solid phases straightforward without removing the culture chamber from the magnetic field owing to a large and open operational space on the culture container. The ability to be processed during levitation also provided the opportunity to fully embed the levitated structures in another phase such as a gel matrix. The sustainability of the culture within a gel matrix ensures that the system can be applied effectively in broad studies including drug response, cell movement and stromal effects.

Mammalian cells exhibit different characteristics for densities depending on their type; for example ~1.044 g/ml for breast cancer cells, ~1.062 g/ml for lung cancer cells (Durmus et al., 2015), ~1.084 g/ml for bone marrow originated stem cells (Sarigil et al., 2019b). Here we have shown that ring magnet-based magnetic levitation system is able to levitate objects with a density ranging from 1.02 to 1.09 g/ml by levitation of particles with known density. Considering the variability of density depending on cellular condition such as type of cell, pathological conditions and differentiation (Neurohr & Amon, 2020), the wide range of applicability of the system has been demonstrated. As models representing levitation of cells with different densities, stem cells, breast cancer cells and adipocytes were self-assembled into 3D structures with preserving cell viability in our system. It was shown that tight and intact 3D cellular units were produced with bone marrow originated stem cells and breast cancer cells and the magnetic levitation system could provide the fusion of biological units composed of stem cells. However, 3D adipocyte clusters were mechanically too unstable for transfer and fusion operations. As the system relies on cell–cell interaction independent of an external mechanical support, the technique is not suitable for natural self-assembly of each cell type. These loose structures may be modified and strengthened by using binary cell mixtures including fibroblasts (Mishriki et al., 2020) and stem cells (Sarigil et al., 2020) to act as an adhesive that promotes intercellular interactions.

One of the most important considerations for the applicability of the levitation system we presented here is the potential toxicity of the paramagnetic medium required for the proper operation. Free form of $Gd^{+}$ causes cytotoxicity by causing a competitive inhibition in $Ca^{2+}$-related biological processes (Sherry et al., 2009). Gadobutrol agent, *which* we used to paramagnetize the medium, is a nonionic macrocyclic Gd chelate that encloses $Gd^{3+}$ in cavity of the cage-like complex and exhibits low disassociation, thus high kinetic stability (Frenzel et al., 2008; Rogosnitzky & Branch, 2016; Schmitt-Willich, 2007). Consistently, we have previously shown that gadobutrol provided the highest cell viability in 2D culture up to the concentration we used in this study, compared to various other ionic or nonionic Gd-based agents containing either linear or macrocyclic ligands (Anil-Inevi et al., 2018). In that previous study, even though gadobutrol appeared as the most effective and the least cytotoxic reagent of magnetic levitation, it still reduced cell viability around 50% after 48 h of exposure at 200 mM concentration. However, 3D culture conditions were expected to increase compound resistance of cells, based on molecular and phenotypic adaptations (Fontoura et al., 2020; Jensen & Teng, 2020; Karadas et al., 2019). Not surprisingly, the present study showed that the viability of cells exposed to gadobutrol in 3D culture for 48 h was higher than in 2D culture by 66% at the same concentration. Lacking molecular-level information, we are unsure if this increase in viability is based on diminished gadobutrol uptake or increased cellular resistance. However, it is clear that the cell viability can decrease below 70% in 3D spheroid cultures due to mass transfer-related conditions (Feng et al., 2017; Gong et al., 2015; Lin & Chang, 2008). Therefore, it is entirely possible that the viability of the system presented here may be further improved by design modifications such as flow integration into the system, and the construction of a microvascular network (Kanczler et al., 2021; Miller et al., 2012). Alternatively, our system can be used only for levitation-based biofabrication but not for levitation-culture, a process that ensures temporal gadobutrol exposure. Even though we can limit the gadobutrol exposure, the long-term effects of the paramagnetic compound especially when cells establish their own ECM may remain as an important issue. For long-term levitation culture potential of our setup, efforts to reduce the concentration of gadobutrol will be important, as long-term effects of paramagnetic agents on cells are still unclear. Gadobutrol cannot naturally enter into the cells (Mohammadi et al., 2014), however, when the cells are cultured long time to form their own ECM, its effect is unclear so the system will also need additional research in terms of cell health that can be affected by various processes such as transchelation (de Schellenberger et al., 2018).

An alternative method to reduce the gadobutrol concentration is by increasing the buoyancy force acting on cells by increasing the surrounding culture medium density. While 100 mM gadobutrol did not provide levitation of mesenchymal stem cells with the original medium density, biofabrication and sustained culture were achieved when the medium density was increased to 1.02 g/ml. By varying the density of the medium between 1.02 and 1.04 g/ml, the required paramagnetic agent concentration for stem cells can probably be lowered further. For cells with a lower density than stem cells, a medium density of 1.02 g/ml could possibly allow levitation below 100 mM. However, increasing the density of the culture medium prolonged the time for the cells to reach equilibrium in levitation. Therefore, further optimization of the culture medium protocol will be necessary for cell-specific long-term applications.

Levitation culture depends on both the physical and biological properties of the living cells. Experimental studies with beads of known density (Figure S1) and simulation results (Figure S9a) have consistently shown that lower $Gd^{3+}$ concentration is sufficient for levitation-based biofabrication with lower density-cells. In addition to the properties of cells in single cell form, the properties they exhibit in the 3D structure also affect levitation culture. The cell–cell interaction between different cell types may result in the formation of tight structures as for stem cells or loose structures as for adipocytes

in this study. Cells that can be packed tightly also fuse better between cellular units, while loosely packed cells (e.g., cancer cells) may fuse slowly or not at all. However, the compaction process may cause decreases in individual cell volume, as in mesenchymal stem cells (75% reduction) (Cesarz & Tamama, 2016; Tsai et al., 2015), and hence, a potential increase in single cell density and decrease in the levitation height of cellular structures. Both cell compaction properties and the culture time are among the factors that can interfere with the viability in the 3D structure. Therefore, further studies are needed for scale-up standardization of levitation culture based on the different cell types.

The process of creating 3D cellular structures by magnetic guidance involves first focusing the single cells homogeneously distributed in the suspension by magnetic force and then gaining a stable architecture of the structure with cell–cell interactions in the focusing region. 3D stable structure formation on the ring magnet-based magnetic levitation system presented herein took more than 10 h regardless of cell type. To shorten this period into couple of hours, the magnetic force applied on the cells was increased by modifying the paramagnetic media, however, the formation process could not be accelerated. Previously a magnetic manipulation method has been described to print 3D cellular structures within 6 h (Mishriki et al., 2019). Unlike our system, this method enabled individual cells to focus on the culture surface rather than levitational assembly. To accelerate cellular aggregation in the ring magnet-based levitation system, the cell focusing process may be accelerated by the physical confinement of the cells in the region close to the low magnetic field (e.g., increasing magnet thickness) or by using binary cell mixtures as an adhesive.

Mini-tissue block fabrication shows great promise in the formation of complex and large 3D anatomical structures. Tissue blocks, which create their own matrix and architecture, show a potential as building blocks for scale-up tissue fabrication. The absence of an external material allows biomaterial-based concerns such as material-induced toxicity and host inflammatory responses to be overcome (Anil et al., 2016, 2020; Murata et al., 2020; Norotte et al., 2009). However, while scaffolding provides void volume for passive diffusion of nutrients, gasses and wastes into the scaffolds to keep the cells alive (Mekala et al., 2014), scaffold-free approaches lack this advantage. Our axial-circular magnetic levitation system may be equipped with a flow system where the bulk liquid phase is continuously refreshed to improve the diffusion between the sphere surface and the liquid phase without distortion of the levitation. In the case of increased spherical size and extended culture periods, the protocol should be tested for the health of cells in the central region before fabrication.

## 5 | CONCLUSIONS

In this study, we proposed an axial-circular magnetic levitation system to remotely manipulate living cells for biofabrication. We verified that the single ring magnet-based magnetic levitation system enabled fabrication of living building blocks and their fusion based on the cellular self-assembly as an alternative to commonly used magnetic levitation systems composed of a culture chamber between two block magnets. The proposed magnetic levitation configuration provides several advantages: (i) Levitation on a single ring magnet eliminates the limit on the height of the culture reservoir, making the system broadly compatible for different types of culture chambers like tubes and cuvettes, and allowing to form and maintain sizeable living structures. (ii) The system provides an open and large operational space allowing for easy and on-site intervention in cell culture such as medium refreshment and adding another structure without distortion of levitation and structures. (iii) Permanent magnets are common and electrical power-independent, therefore the design enables straightforward, simple and low-cost installation and operation. (iv) Label-, scaffold- and nozzle-free nature of the protocol allows for manufacturing of living constructs that is rapid, natural-like and free from mechanical stress. The platform presented here may be improved by automation with a perfusion system for a continuous fabrication and by providing on-site monitoring at high magnification under microscope using mirrors. The system offers wide range applications including biofabrication of scale-up complex structures and of tissue models for drug testing and cancer research by operating in batch or continuous mode.

## ACKNOWLEDGMENTS

Financial support by The Scientific and Technological Research Council of Turkey (119M755) is gratefully acknowledged.

## DATA AVAILABILITY STATEMENT

The data that support the findings of this study are available from the corresponding author upon reasonable request.

## ORCID

*Muge Anil-Inevi* http://orcid.org/0000-0003-2854-3472
*Kerem Delikoyun* http://orcid.org/0000-0002-3294-049X
*Gulistan Mese* http://orcid.org/0000-0003-0458-8684
*H. Cumhur Tekin* http://orcid.org/0000-0002-5758-5439
*Engin Ozcivici* http://orcid.org/0000-0003-4464-0475

## REFERENCES

Anil, M., Ayyildiz-Tamis, D., Tasdemir, S., Sendemir-Urkmez, A., & Gulce-Iz, S. (2016). Bioinspired materials and biocompatibility. In M. Bououdina (Eds.), *Emerging research on bioinspired materials engineering* (pp. 294–322). IGI Global.

Anil-Inevi, M., Sağlam-Metiner, P., Kabak, E. C., & Gulce-Iz, S. (2020). Development and verification of a three-dimensional (3D) breast cancer tumor model composed of circulating tumor cell (CTC) subsets. *Molecular Biology Reports*, *47*(1), 97–109.

Anil-Inevi, M., Yalcin-Ozuysal, O., Sarigil, O., Mese, G., Ozcivici, E., Yaman, S. & Tekin, H. C. (2019a). Biofabrication of Cellular Structures Using Weightlessness as a Biotechnological Tool. 2019 9th International Conference on Recent Advances in Space Technologies (RAST), IEEE, 929–931.

Anil-Inevi, M., Yaman, S., Yildiz, A. A., Mese, G., Yalcin-Ozuysal, O., Tekin, H. C., & Ozcivici, E. (2018). Biofabrication of in situ self assembled 3D cell cultures in a weightlessness environment generated using magnetic levitation. *Scientific Reports*, *8*(1), 1–10.

Anil-Inevi, M., Yilmaz, E., Sarigil, O., Tekin, H. C. & Ozcivici, E. (2019b). Single cell densitometry and weightlessness culture of mesenchymal stem cells using magnetic levitation. 15–25

Baday, M., Ercal, O., Sahan, A. Z., Sahan, A., Ercal, B., Inan, H., & Demirci, U. (2019). Density based characterization of mechanical cues on cancer cells using magnetic levitation. *Advanced Healthcare Materials*, *8*(10), 1801517.

Castro, E., & Mano, J. F. (2013). Magnetic force-based tissue engineering and regenerative medicine. *Journal of Biomedical Nanotechnology*, *9*, 1129–1136.

Cesarz, Z. & Tamama, K. (2016). Spheroid culture of mesenchymal stem cells, Stem cells international 2016

Chen, P., Huang, Y.-Y., Hoshino, K., & Zhang, J. X. J. (2015). Microscale magnetic field modulation for enhanced capture and distribution of rare circulating tumor cells. *Scientific Reports*, *5*(1), 8745.

Durmus, N. G., Tekin, H. C., Guven, S., Sridhar, K., Yildiz, A. A., Calibasi, G., Ghiran, I., Davis, R. W., Steinmetz, L. M., & Demirci, U. (2015). Magnetic levitation of single cells. *Proceedings of the National Academy of Sciences*, *112*(28), E3661–E3668.

Feng, J., Mineda, K., Wu, S.-H., Mashiko, T., Doi, K., Kuno, S., Kinoshita, K., Kanayama, K., Asahi, R., & Sunaga, A. (2017). An injectable non-cross-linked hyaluronic-acid gel containing therapeutic spheroids of human adipose-derived stem cells. *Scientific Reports*, *7*(1), 1–13.

Fontoura, J. C., Viezzer, C., Dos Santos, F. G., Ligabue, R. A., Weinlich, R., Puga, R. D., Antonow, D., Severino, P., & Bonorino, C. (2020). Comparison of 2D and 3D cell culture models for cell growth, gene expression and drug resistance. *Materials Science and Engineering: C*, *107*, 110264.

Frenzel, T., Lengsfeld, P., Schirmer, H., Hütter, J., & Weinmann, H.-J. (2008). Stability of gadolinium-based magnetic resonance imaging contrast agents in human serum at 37 C. *Investigative Radiology*, *43*(12), 817–828.

Ge, S., & Whitesides, G. M. (2018). "Axial" magnetic levitation using ring magnets enables simple density-based analysis, separation, and manipulation. *Analytical Chemistry*, *90*(20), 12239–12245.

Gong, X., Lin, C., Cheng, J., Su, J., Zhao, H., Liu, T., Wen, X., & Zhao, P. (2015). Generation of multicellular tumor spheroids with microwell-based agarose scaffolds for drug testing. *PLoS One*, *10*(6), e0130348.

Haisler, W. L., Timm, D. M., Gage, J. A., Tseng, H., Killian, T., & Souza, G. R. (2013). Three-dimensional cell culturing by magnetic levitation. *Nature Protocols*, *8*(10), 1940–1949.

Ino, K., Okochi, M., & Honda, H. (2009). Application of magnetic force-based cell patterning for controlling cell–cell interactions in angiogenesis. *Biotechnology and Bioengineering*, *102*(3), 882–890.

Jensen, C., & Teng, Y. (2020). Is it time to start transitioning from 2D to 3D cell culture? *Frontiers in Molecular Biosciences*, *7*, 33.

Jeong, Y. G., Lee, J. S., Shim, J. K., & Hur, W. (2016). A scaffold-free surface culture of B16F10 murine melanoma cells based on magnetic levitation. *Cytotechnology*, *68*(6), 2323–2334.

Jing, Y., Mal, N., Williams, P. S., Mayorga, M., Penn, M. S., Chalmers, J. J., & Zborowski, M. (2008). Quantitative intracellular magnetic nanoparticle uptake measured by live cell magnetophoresis, The. *FASEB Journal*, *22*(12), 4239–4247.

Delikoyun, K., Yaman, S., Yilmaz, E., Sarigil, O., Anil-Inevi, M., Telli, K., Yalcin-Ozuysal, O., Ozcivici, E., & Tekin, H. C. (2021). HologLev: A hybrid magnetic levitation platform integrated with lensless holographic microscopy for density-based cell analysis. *ACS Sensors*, *6*(6), 2191–2201.

Kanczler, J. M., Wells, J. A., & Oreffo, R. O. (2021). Endothelial cells: Co-culture spheroids. In D. Ribatti & *V. Morphogenesis* (Eds.), *Methods in molecular biology* (pp. 47–56). Humana.

Karadas, O., Mese, G., & Ozcivici, E. (2019). Cytotoxic tolerance of healthy and cancerous bone cells to anti-microbial phenolic compounds depend on culture conditions. *Applied Biochemistry and Biotechnology*, *188*(2), 514–526.

Lin, R. Z., & Chang, H. Y. (2008). Recent advances in three-dimensional multicellular spheroid culture for biomedical research, Biotechnology Journal: Healthcare Nutrition. *Technology*, *3*(9-10), 1172–1184.

Mattix, B., Olsen, T. R., Gu, Y., Casco, M., Herbst, A., Simionescu, D. T., Visconti, R. P., Kornev, K. G., & Alexis, F. (2014). Biological magnetic cellular spheroids as building blocks for tissue engineering. *Acta Biomaterialia*, *10*(2), 623–629.

Mekala, N. K., Baadhe, R. R., & Potumarthi, R. (2014). Mass transfer aspects of 3D cell cultures in tissue engineering. *Asia-Pacific Journal of Chemical Engineering*, *9*(3), 318–329.

Menasche, B. L., Crisman, L., Gulbranson, D. R., Davis, E. M., Yu, H., & Shen, J. (2019). Fluorescence activated cell sorting (FACS) in genome-wide genetic screening of membrane trafficking. *Current Protocols in Cell Biology*, *82*(1), e68.

Miller, J. S., Stevens, K. R., Yang, M. T., Baker, B. M., Nguyen, D.-H. T., Cohen, D. M., Toro, E., Chen, A. A., Galie, P. A., & Yu, X. (2012). Rapid casting of patterned vascular networks for perfusable engineered three-dimensional tissues. *Nature Materials*, *11*(9), 768–774.

Mirica, K. A., Ilievski, F., Ellerbee, A. K., Shevkoplyas, S. S., & Whitesides, G. M. (2011). Using magnetic levitation for three dimensional self-assembly. *Advanced Materials*, *23*(36), 4134–4140.

Mirica, K. A., Phillips, S. T., Mace, C. R., & Whitesides, G. M. (2010). Magnetic levitation in the analysis of foods and water. *Journal of Agricultural and Food Chemistry*, *58*(11), 6565–6569.

Mirica, K. A., Shevkoplyas, S. S., Phillips, S. T., Gupta, M., & Whitesides, G. M. (2009). Measuring densities of solids and liquids using magnetic levitation: fundamentals. *Journal of the American Chemical Society*, *131*(29), 10049–10058.

Mishriki, S., Aithal, S., Gupta, T., Sahu, R. P., Geng, F., & Puri, I. K. (2020). Fibroblasts accelerate formation and improve reproducibility of 3D cellular structures printed with magnetic assistance. *Research; A Journal Of Science And Its Applications*, *2020*(2020), 1–15.

Mishriki, S., Fattah, A. A., Kammann, T., Sahu, R., Geng, F., & Puri, I. (2019). Rapid magnetic 3D printing of cellular structures with MCF-7 cell inks. *Research; A Journal of Science And its Applications*, *2019*, 9854593.

Mohammadi, E., Amanlou, M., Ebrahimi, S. E. S., Hamedani, M. P., Mahrooz, A., Mehravi, B., Abd Emami, B., Aghasadeghi, M. R., Bitarafan-Rajabi, A., & Akbar, H. R. P. A. (2014). Cellular uptake, imaging and pathotoxicological studies of a novel Gd [III]–DO3A-butrol nano-formulation. *RSC Advances*, *4*(86), 45984–45994.

Morrison, W. A., Marre, D., Grinsell, D., Batty, A., Trost, N., & O'Connor, A. J. (2016). Creation of a large adipose tissue construct in humans using a tissue-engineering chamber: A step forward in the clinical application of soft tissue engineering. *EBioMedicine*, *6*, 238–245.

Murata, D., Arai, K., & Nakayama, K. (2020). Scaffold-free bio-3D printing using spheroids as "Bio-Inks" for tissue (Re-) construction and drug response tests, advanced healthcare. *Materials*, 1901831.

Nam-Trung, N. (2012). Micro-magnetofluidics: Interactions between magnetism and fluid flow on the microscale. *Microfluidics and Nanofluidics*, *12*, 1–16.

Neurohr, G. E., & Amon, A. (2020). Relevance and regulation of cell density. *Trends in Cell Biology*, *30*(3), 213–225.

Norotte, C., Marga, F. S., Niklason, L. E., & Forgacs, G. (2009). Scaffold-free vascular tissue engineering using bioprinting. *Biomaterials*, *30*(30), 5910–5917.

Pamme, N. (2006). Magnetism and microfluidics. *Lab on a Chip*, *6*(1), 24–38.

Pan, Y., Du, X., Zhao, F., & Xu, B. (2012). Magnetic nanoparticles for the manipulation of proteins and cells. *Chemical Society Reviews*, *41*(7), 2912–2942.

Parfenov, V. A., Koudan, E. V., Bulanova, E. A., Karalkin, P. A., Pereira, F. D., Norkin, N. E., Knyazeva, A. D., Gryadunova, A. A., Petrov, O. F., & Vasiliev, M. M. (2018). Scaffold-free, label-free and

nozzle-free biofabrication technology using magnetic levitational assembly. *Biofabrication*, *10*(3), 034104.

Parfenov, V. A., Koudan, E. V., Krokhmal, A. A., Annenkova, E. A., Petrov, S. V., Pereira, F. D., Karalkin, P. A., Nezhurina, E. K., Gryadunova, A. A., & Bulanova, E. A. (2020). Biofabrication of a functional tubular construct from tissue spheroids using magnetoacoustic levitational directed assembly, advanced healthcare. *Materials*, *9*(24), 2000721.

Parfenov, V. A., Mironov, V. A., van Kampen, K. A., Karalkin, P. A., Koudan, E. V., Pereira, F. D., Petrov, S. V., Nezhurina, E. K., Petrov, O. F., & Myasnikov, M. I. (2020). Scaffold-free and label-free biofabrication technology using levitational assembly in a high magnetic field. *Biofabrication*, *12*(4), 045022.

Park, I. S., Jin, R. L., Oh, H. J., Truong, M. D., Choi, B. H., Park, S. H., Park, D. Y., & Min, B. H. (2019). Sizable scaffold-free tissue-engineered articular cartilage construct for cartilage defect repair. *Artificial Organs*, *43*(3), 278–287.

Van Peer, G., Mestdagh, P., & Vandesompele, J. (2012). Accurate RT-qPCR gene expression analysis on cell culture lysates. *Scientific Reports*, *2*, 222.

Robert, D., Pamme, N., Conjeaud, H., Gazeau, F., Iles, A., & Wilhelm, C. (2011). Cell sorting by endocytotic capacity in a microfluidic magnetophoresis device. *Lab on a Chip*, *11*(11), 1902–1910.

Rogosnitzky, M., & Branch, S. (2016). Gadolinium-based contrast agent toxicity: A review of known and proposed mechanisms. *BioMetals*, *29*(3), 365–376.

Sarigil, O., Anil-Inevi, M., Yilmaz, E., Cagan, M., Mese, G., Tekin, H. C. & Ozcivici, E. (2019a). Application of Magnetic Levitation Induced Weightlessness to Detect Cell Lineage. 2019 9th International Conference on Recent Advances in Space Technologies (RAST), IEEE, 933–935.

Sarigil, O., Anil-Inevi, M., Yilmaz, E., Mese, G., Tekin, H. C., & Ozcivici, E. (2019b). Label-free density-based detection of adipocytes of bone marrow origin using magnetic levitation. *Analyst*, *144*(9), 2942–2953.

Sarigil, O., Anil-Inevi, M., Firatligil-Yildirir, B., Unal, Y. C., Yalcin-Ozuysal, O., Mese, G., Tekin, H. C., & Ozcivici, E. (2020). Scaffold-free biofabrication of adipocyte structures with magnetic levitation. *Biotechnology and Bioengineering*, *118*, 1127–1140.

de Schellenberger, A. A., Bergs, J., Sack, I., & Taupitz, M. (2018). The extracellular matrix as a target for biophysical and molecular magnetic resonance imaging. In I. Sack & T. Schaeffter (Eds.), *Quantification of biophysical parameters in medical imaging* (pp. 123–150). Springer.

Schmitt-Willich, H. (2007). Stability of linear and macrocyclic gadolinium based contrast agents. *The British Journal of Radiology*, *80*(955), 581–582.

Shen, Y., Vignali, P., & Wang, R. (2017). Rapid profiling cell cycle by flow cytometry using concurrent staining of DNA and mitotic markers. *Bio Protoc*, *7*):e2517.

Sherry, A. D., Caravan, P., & Lenkinski, R. E. (2009). Primer on gadolinium chemistry. *Journal of Magnetic Resonance Imaging: An Official Journal of the International Society for Magnetic Resonance in Medicine*, *30*(6), 1240–1248.

Simon, M., & Geim, A. (2000). Diamagnetic levitation: Flying frogs and floating magnets. *Journal of Applied Physics*, *87*(9), 6200–6204.

Souza, G. R., Molina, J. R., Raphael, R. M., Ozawa, M. G., Stark, D. J., Levin, C. S., Bronk, L. F., Ananta, J. S., Mandelin, J., & Georgescu, M.-M. (2010). Three-dimensional tissue culture based on magnetic cell levitation. *Nature Nanotechnology*, *5*(4), 291–296.

Subramaniam, A. B., Yang, D., Yu, H.-D., Nemiroski, A., Tricard, S., Ellerbee, A. K., Soh, S., & Whitesides, G. M. (2014). Noncontact orientation of objects in three-dimensional space using magnetic levitation. *Proceedings of the National Academy of Sciences*, *111*(36), 12980–12985.

Tarn, M. D., Peyman, S. A., Robert, D., Iles, A., Wilhelm, C., & Pamme, N. (2009). The importance of particle type selection and temperature control for on-chip free-flow magnetophoresis. *Journal of Magnetism and Magnetic Materials*, *321*(24), 4115–4122.

Tasoglu, S., Khoory, J. A., Tekin, H. C., Thomas, C., Karnoub, A. E., Ghiran, I. C., & Demirci, U. (2015a). Levitational image cytometry with temporal resolution. *Advanced Materials*, *27*(26), 3901–3908.

Tasoglu, S., Yu, C. H., Liaudanskaya, V., Guven, S., Migliaresi, C., & Demirci, U. (2015b). Magnetic levitational assembly for living material fabrication. *Advanced Healthcare Materials*, *4*(10), 1469–1476.

Tocchio, A., Durmus, N. G., Sridhar, K., Mani, V., Coskun, B., El Assal, R., & Demirci, U. (2018). Magnetically guided self-assembly and coding of 3D living architectures. *Advanced Materials*, *30*(4), 1705034.

Tsai, A.-C., Liu, Y., Yuan, X., & Ma, T. (2015). Compaction, fusion, and functional activation of three-dimensional human mesenchymal stem cell aggregate. *Tissue Engineering*, *Part A 21*(9-10), 1705–1719.

Türker, E., Demirçak, N., & Arslan-Yildiz, A. (2018). Scaffold-free three-dimensional cell culturing using magnetic levitation. *Biomaterials Science*, *6*(7), 1745–1753.

Whatley, B. R., Li, X., Zhang, N., & Wen, X. (2014). Magnetic-directed patterning of cell spheroids. *Journal of Biomedical Materials Research. Part A*, *102*(5), 1537–1547.

Winkleman, A., Gudiksen, K. L., Ryan, D., Whitesides, G. M., Greenfield, D., & Prentiss, M. (2004). A magnetic trap for living cells suspended in a paramagnetic buffer. *Applied Physics Letters*, *85*(12), 2411–2413.

Yaman, S., Anil-Inevi, M., Ozcivici, E., & Tekin, H. C. (2018). Magnetic force-based microfluidic techniques for cellular and tissue bioengineering. *Frontiers in Bioengineering and Biotechnology*, *6*, 192.

Zeng, L., Qiu, L., Yang, X.-T., Zhou, Y.-H., Du, J., Wang, H.-Y., Sun, J.-H., Yang, C., & Jiang, J.-X. (2015). Isolation of lung multipotent stem cells using a novel microfluidic magnetic activated cell sorting system. *Cell Biology International*, *39*(11), 1348–1353.

Zhang, C., Zhao, P., Gu, F., Xie, J., Xia, N., He, Y., & Fu, J. (2018). Single-ring magnetic levitation configuration for object manipulation and density-based measurement. *Analytical Chemistry*, *90*(15), 9226–9233.

Zhang, C., Zhao, P., Gu, F., Zhang, X., Xie, J., He, Y., Zhou, H., Fu, J., & Turng, L.-S. (2020). Axial-circular magnetic levitation: A three-dimensional density measurement and manipulation approach. *Analytical Chemistry*, *22*, 4197–4206.

Zhang, C., Zhao, P., Tang, D., Xia, N., Zhang, X., Nie, J., Gu, F., Zhou, H., & Fu, J. (2019). Axial magnetic levitation: A high-sensitive and maneuverable density-based analysis device. *Sensors and Actuators B: Chemical*, *304*, 127362.

Zhao, W., Cheng, R., Miller, J. R., & Mao, L. (2016). Label-free microfluidic manipulation of particles and cells in magnetic liquids. *Advanced Functional Materials*, *26*(22), 3916–3932.

## SUPPORTING INFORMATION

Additional supporting information may be found in the online version of the article at the publisher's website.

**How to cite this article:** Anil-Inevi, M., Delikoyun, K., Mese, G., Tekin, H. C., & Ozcivici, E. (2021). Magnetic levitation assisted biofabrication, culture, and manipulation of 3D cellular structures using a ring magnet based setup. *Biotechnology and Bioengineering*, 118, 4771–4785. https://doi.org/10.1002/bit.27941